Integrated Intelligent Computing Paradigm for Nonlinear Multi-Singular Third Order Emden-Fowler Equation

Zulqurnain Sabir[1,*], Muhammad Umar[2], Juan L.G. Guirao[3], Muhammad Shoaib[4], Muhammad Asif Zahoor Raja[5]

[1]Department of Mathematics and Statistics, Hazara University, Mansehra, Pakistan

Emails: zulqurnain_maths@hu.edu.pk

[2]Department of Mathematics and Statistics, Hazara University, Mansehra, Pakistan
Emails: umar_maths@hu.edu.pk, humar922015@gmail.com
[3]Department of Applied Mathematics and Statistics, Technical University of Cartagena, Hospital de Marina 30203-Cartagena, Spain
Email: juan.garcia@upct.es

[4]Department of Mathematics, COMSATS University Islamabad, Attock Campus, Attock 43600, Pakistan
dr.shoaib@cuiatk.edu.pk

[5]Department of Electrical and Computer Engineering, COMSATS University Islamabad, Attock Campus, Attock 43600, Pakistan
Email: Muhammad.asif@ciit-attock.edu.pk

Abstract: In this study, an advance computational intelligence scheme is applied to solve third order nonlinear multiple singular systems represented with third order Emden-Fowler differential equation (EFDE) by exploiting the efficacy of artificial neural networks (ANNs), genetic algorithms (GAs) and active-set algorithm (ASA). ANN is used to discretize the EFDE to formulated mean squared error based fitness function. The optimization task for nonlinear multi-singular system is performed by integrated competency GA and ASA, i.e., GA-ASA. The efficiency of the designed scheme is examined by solving five different variants of the singular model to check the effectiveness, reliability and significance of the proposed technique. The statistical investigations are also performed to authenticate the precision, accuracy and convergence.

Keywords: Nonlinear Emden-Fowler equation, Artificial Neural Networks, Statistical Analysis, Genetic Algorithms, Singular Systems, Active-Set Algorithm, Hybrid Computing

1. Introduction

Astrophysicist Jonathan Homer Lane [1] and Robert Emden [2] first time introduced nonlinear singular Lane-Emden model working on thermal performance of a spherical cloud of gas and classical law of thermodynamics [3]. The singular models designate a variety of phenomena in physical science [4], density profile of gaseous star [5], catalytic diffusion reactions [6], isothermal gas spheres [7], catalytic diffusion reactions [8], stellar structure [9], electromagnetic theory [10], mathematical physics [11], classical and quantum mechanics [12], oscillating magnetic fields [13], isotropic continuous media [14], dusty fluid models [15] and morphogenesis [16].

To find the solution of singular models are always very challengeable and hard to handle due to the singularity at the origin. There are only few numerical and analytic existing techniques to tackle such a nonlinear singular model. To mention few techniques to solve the singular models, Bender et al [17] proposed a perturbative technique, Shawagfeh [18] suggested Adomian decomposition method (ADM), Wazwaz [19] also applied ADM to avoid the difficulty of singularity, Liao [20] applied an analytic algorithm to avoid the singularity, Parand and Razzaghi [21] developed a numerical scheme to present the solution, Nouh [22] applied power series solution by using Pade approximation techniqueas well as Euler-Abel transformationand Mandelzweigand along with Tabakin [23] developed Bellman and Kalabas quasi linearization method. All these techniques have their own performance, accuracy and efficiency, as well as imperfections over one another. The heuristic techniques based on stochastic solvers optimize with linear/nonlinear models by manipulating the artificial neural networks (ANNs) and practical adaptation of evolutionary computing applications [24-26]. Some possible recent applications are Thomas-Fermi atom's model [27], prey-predator models [28], plasma physics problems [29], transistor-level uncertainty quantification [30], heartbeat model [31], human physiology [32], control systems [33], cell biology [34], power [35] and energy [36].The intention of the present study is to perform the comprehensive form of the singular Emden-Fowler model and its numerical results to develop the system understanding using the stochastic technique.

The generic form of the Emden-Fowler equation is written as [37]:

$$
\begin{aligned}
&y'''(t)+\left(\frac{2p}{t}\right)y''(t)+\frac{p(p-1)}{t^2}y'(t)+f(t)g(y)=0,\\
&y(0)=y_0,\ y'(0)=0,\ \ y''(0)=0.
\end{aligned}
\qquad \textbf{(1)}
$$

The aim of the present study is to solve the equation (1) using integrated intelligent computing paradigm based on the artificial neural networks (ANNs) optimized with genetic algorithms (GAs) refined by the active-set algorithm (ASA), i.e., ANN-GA-ASA. The major features of the proposed solver ANN-GA-ASA are briefly given below:

- A novel application of integrated intelligent computing paradigm ANN-GA-ASA for finding the solutions of nonlinear multi-singular models governed with third order Emden-Fowler equation.
- The consistent matched outcomes of the proposed scheme ANN-GA-ASA with reference solutions of the Emden-Fowler system established the accuracy, convergence and stability.
.
- Validation of the performance is ascertained through statistical observations in terms of mean absolute deviation, Theil's inequality coefficient and Nash Sutcliffe efficiency.

The rest of the paper is organized as follows: In section 2, the proposed methodology is discussed; In 3rd section, the mathematical form of performance operators is discussed; In section 4, the detailed result and discussion are provided. Finally, conclusion are drawn in the last section.

2. Proposed Methodology

The proposed framework for presenting the solution of model (1) is divided in two portions. Firstly, by introducing the procedure for formulation of an error-based fitness function and secondly, the combination of GA-ASA is presented to optimize the fitness function for system (1).

2.1 ANN modeling

The variety of ANNs models introduced by research community for the solutions of linear and nonlinear problems arising in different fields [38-40]. The feed-forward ANN models based procedure for approximating solutions and their respective m^{th} order derivatives are mathematically presented as:

$$\hat{y}(t)=\sum_{j=1}^{n}\alpha_j h(\delta_j t+\beta_j), \quad \textbf{(2)}$$

$$\hat{y}^{(m)}(t)=\sum_{j=1}^{n}\alpha_j h^{(m)}(\delta_j t+\beta_j), \quad \textbf{(3)}$$

Where α_j, β_j and δ_j are the j^{th} components of vectors $\boldsymbol{\alpha}$, $\boldsymbol{\beta}$ and $\boldsymbol{\delta}$, respectively, while m shows the derivative order. The log-sigmoid function $h(t)\ =\left(1+\exp(-t)\right)^{-1}$ and its derivative are used as an activation functions in the networks. The updated form of the above network is given as:

$$\hat{y}(t)=\sum_{j=1}^{n}\alpha_j\left(1+e^{-(\delta_j t+\beta_j)}\right)^{-1}, \quad \textbf{(4)}$$

$$\hat{y}^{(m)}(t)=\sum_{j=1}^{n}\alpha_j\frac{d^m}{dt^m}\left(\left(1+e^{-(\delta_j t+\beta_j)}\right)^{-1}\right). \quad \textbf{(5)}$$

In case of Emden-Fowler equation (1), the expression for high order derivative in ANN formulations is given as:

$$\tilde{y}'''(t)=\sum_{j=1}^{n}\alpha_j\delta_j{}^3\left(\frac{6e^{-3(\delta_j t+\beta_j)}}{\left(1+e^{-(\delta_j t+\beta_j)}\right)^4}-\frac{6e^{-2(\delta_i t+\beta_i)}}{\left(1+e^{-(\delta_j t+\beta_j)}\right)^3}+\frac{e^{-(\delta_i t+\beta_i)}}{\left(1+e^{-(\delta_j t+\beta_j)}\right)^2}\right) \quad \textbf{(6)}$$

The combination of the equations (4) to (6) is exploited for the fitness function formulation of equation (1) in mean squared error sense as:

$$\varepsilon=\varepsilon_1+\varepsilon_2, \quad \textbf{(7)}$$

$$\varepsilon_1 = \frac{1}{N}\sum_{k=1}^{N}\left(\hat{y}_k''' + 2pt_k^{-1}\hat{y}_k'' + p(p-1)t_k^{-2}\hat{y}_k' + f_k g(\hat{y}_k)\right)^2, \quad \textbf{(8)}$$

$$\varepsilon_2 = \frac{1}{2}((\hat{y}_0 - A)^2 + (\hat{y}_0')^2 + (\hat{y}_0'')^2), \quad \textbf{(9)}$$

where ε_1 and ε_2 are the fitness/error functions associated with the model equation (1) and its initial conditions, respectively, while $N = 1/h,\ \hat{y}_k = \hat{y}(t_k),\ t_k = kh,\ f_k = f(t_k)$. An appropriate optimization procedure is adopted for learning of weight vector $W = [\boldsymbol{\alpha}, \boldsymbol{\delta}, \boldsymbol{\beta}]$, such that error based fitness function (7) approaches to optimal zero value.

2.2 Optimization procedure

The weights of ANNs are trained by manipulating the strength of integrated meta-heuristic computing procedure based on GAs supported with ASA, i.e., GA-ASA. The graphical abstract of present designed methodology for solving equation (1) is shown in Fig. 1.

Global search efficacy of GAs, introduced by Holand in early 1970's [41-42], is exploited for finding the weight vector *W* of ANN. Population formulation with candidate solution or individual in GAs is performed using the bounded real numbers. While, each candidate solution or individual has elements equal to unknown weights in ANN models. GAs operate with its major operators based on crossover, selection,mutation and elitism procedures and has been used in many applications recently, for instance, optimize heterogeneous bin packing [43], emergency humanitarian logistics scheduling [44], cost optimization for a multi-energy source building [45], traveling salesman problem [46], optimal set of overlapping clusters [47], building envelope design for residential buildings [48], nanofluid flow [49], optimization of queens problem [50], implementation of intrusion detection system [51], determination of glass transitions in boiled candies [52] and to design the military surveillance nets [53].

The optimized parameters of GA converge faster by the hybridization procedure with the appropriate local search method using the GAs global best values as an initial weight. Therefore, efficient local search method based on ASA is used of rapid fine-tuning of parameters. In recent years, ASA is used in many applications e.g., scalable elastic net subspace clustering [54], solution of least squares problems [55], distributed model predictive control [56], transportation of discrete network design bi-level problem [57] and in the solution of ball/sphere constrained optimization problems [58]. In the present work, the hybrid of GA-ASA is used to find the designed variables for solving the third order singular model. the detailed pseudocode of GA-ASA is tabulated in Table 1

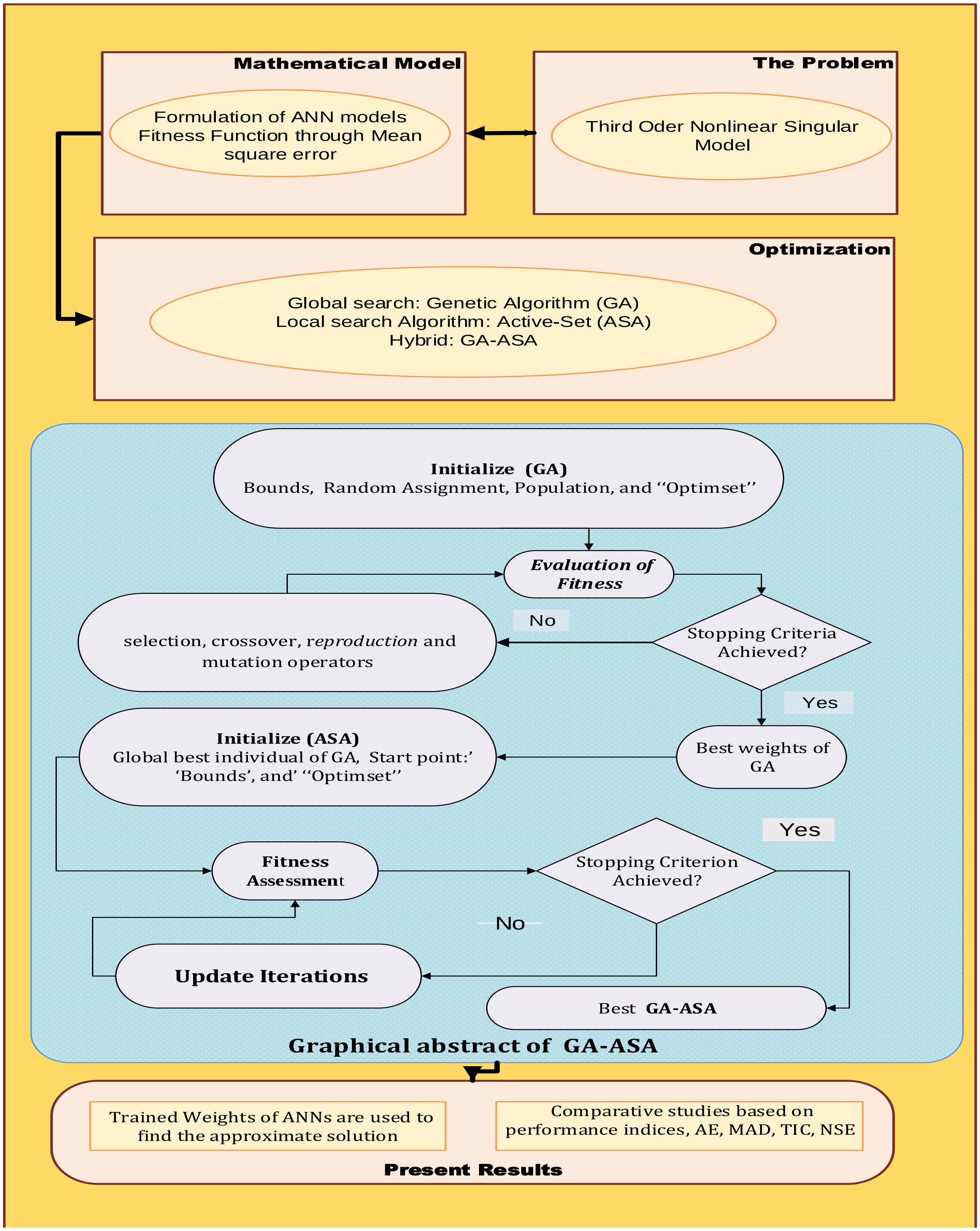

Figure 1: Framework of proposed methodology for solving the nonlinear third order singular Emden Fowler model

Table 1: Pseudo-code of optimization scheme of GA-ASA

Genetic Algorithms procedure started

Inputs:

The chromosome with equal number of unknown elements of the Networks as: $\boldsymbol{W}=[\boldsymbol{\alpha}, \boldsymbol{\delta}, \boldsymbol{\beta}]$, where

$\boldsymbol{\alpha}=[\alpha_1,\alpha_2,\alpha_3,...,\alpha_m]$, $\boldsymbol{\delta}=[\delta_1,\delta_2,\delta_3,...,\delta_m]$ and

$\boldsymbol{\beta}=[\beta_1,\beta_2,\beta_{3,}...,\beta_m]$

Population: A set of chromosomes represented as:

$\boldsymbol{P}=[\boldsymbol{W}_1, \boldsymbol{W}_2,,...,\boldsymbol{W}_n]^t$, $\boldsymbol{w}_i=[\boldsymbol{\alpha}_i, \boldsymbol{\delta}_i, \boldsymbol{\beta}_i]^t$

Output: The Best Global weights trained by GAs $\boldsymbol{W}_{\mathbf{B.ga}}$

Initialization

Create $\boldsymbol{W}$ vector of real bounded numbers to denote a chromosome. Set of $\boldsymbol{W}$ to make an initial $\boldsymbol{P}$. Set the values of declarations and Generation of 'GA' and 'gaoptimset' routines.

Fitness formulation

Achieved the fitness ε in $\boldsymbol{P}$ for all $\boldsymbol{W}$ using equation (5) to (7)

Termination

Terminate the procedure to attain one of the following

- 'Fitness e $\rightarrow 10^{-18}$',
- 'TolFun = TolCon$\rightarrow 10^{-18}$', 'TolX $\rightarrow 10^{-20}$',
- 'StallGenLimit $\rightarrow$120', 'Generations$\rightarrow$ 80'
- 'PopulationSize $\rightarrow$ 300'
- gaoptimset and GA functions are taken as default

Go to step **storage**, when termination criteria meets,

Ranking

Ranked each $\boldsymbol{W}$ of $\boldsymbol{P}$ for quality of the fitness ε

Reproduction

- 'Selection: @selectionuniform'.
- 'Crossover: @crossoverheuristic'.
- 'Mutations: @mutationadaptfeasible'.
- 'Elitism: For best ranked individuals of $\boldsymbol{P}$,

Continue from "**fitness evaluation**" step'

Storage

Save the weight vector $\boldsymbol{W}_{\mathbf{B.ga}}$, fitness evaluation ε, time generation and function counts for GAs

End Genetic algorithms

ASA Procedure Start

Inputs

Start point: $\boldsymbol{W}_{\mathbf{B.ga}}$

Output

GA-ASA best weights are denotes as $\boldsymbol{W}_{\mathbf{GA.ASA}}$

Initialize

Bounded constraints, assignments, total number of iterations and other decelerations

```
    Terminate
          Algorithm stops for any conditions meet:
          'Fitness e ≤ 10^-16, Iterations = 1000, TolX ≤ 10^-20
          TolFun=TolCon ≤ 10^-18 and MaxFunEvals ≤ 220000
          While (Required termination satisfied)
          Fitness calculation
          To evaluate the fitness value ε of the weight
          vector W by using equations (5) to (7)
          Adjustments
          Invoking "fmincon" for the ASA. Adapt weight
          vector W for each generation of ASA. Compute
          fitness value of improved weight vector W again
          by using equations(5)to(7)
    Accumulate
          Store the values of weight vectorW_GA.ASA,fitness ε,
          time t, number of generations and function counts
    for the recent runs of ASA.
ASA Procedure End
Data Generations
Repeat 100 times the GA-ASA process to get an enormous data-set
of the optimization variables of ANNs to solve third order
singular model (1)
```

3. Performance measures

The performance measures of mean absolute deviation (MAD), Nash Sutcliff efficiency (NSE) and Theil's inequality coefficient (TIC) are used in this study.

The mathematical description of MAD, TIC and ENSE by means of the exact/true solution y and approximate/calculated solution $\hat{y}$ are provided below:

$$\text{MAD}=\frac{1}{n}\sum_{m=1}^{n}\left|y_m-\hat{y}_m\right|, \tag{10}$$

$$\text{TIC}=\frac{\sqrt{\frac{1}{n}\sum_{m=1}^{n}\left(y_m-\hat{y}_m\right)^2}}{\left(\sqrt{\frac{1}{n}\sum_{m=1}^{n}y_m^2}+\sqrt{\frac{1}{n}\sum_{m=1}^{n}\hat{y}_m^2}\right)} \tag{11}$$

$$\text{NSE}=\left\{1-\frac{\sum_{m=1}^{n}\left(y_m-\hat{y}_m\right)^2}{\sum_{m=1}^{n}\left(y_m-\bar{y}_m\right)^2},\right. \qquad \bar{y}_m=\frac{1}{n}\sum_{m=1}^{n}y_m \tag{12}$$

$$\text{E}_{NSE}=1\text{-NSE} \tag{13}$$

4. Results and discussions

The detailed results and discussion for five cases of nonlinear singular system are presented in this section

Case-1:

Consider the nonlinear Emden-Fowler equation by putting $p=1$ and $f(t)g(y)=-\frac{9}{8}(t^6+8)y^{-5}$ in equation (1) written as

$$\begin{aligned}
&\mathrm{y}'''(\mathrm{t})+\left(\frac{2}{t}\right)y''(t)-\frac{9}{8}(8+t^6)y^{-5}=0 \\
&y(0)=1,\ y'(0)=0,\ y''(0)=0.
\end{aligned} \tag{14}$$

The exact/true form of above equation (14) is $\sqrt{1+t^3}$ and the fitness/error function of above equation is given below:

$$\varepsilon=\frac{1}{N}\sum_{m=1}^{N}\left(8t_m\hat{y}'''(t_m)+16\hat{y}''(t_m)-9t_m(t_m^6+8)\hat{y}^{-5}\right)^2+\frac{1}{3}\left(\left(\hat{y}_0-1\right)^2+\left(\hat{y}_0'\right)^2+\left(\hat{y}_0''\right)\right) \tag{15}$$

Case-2:

Consider the third order Emden-Fowler model by using $p=2$ and $f(t)g(y)=-9(3t^6+10t^3+4)y$ in equation (1) becomes as

$$\begin{aligned}
&\mathrm{y}'''(\mathrm{t})+\left(\frac{4}{t}\right)y''(t)+\left(\frac{2}{t^2}\right)y'(t)-9(4+10t^3+3t^6)y=0 \\
&y(0)=1,\ y'(0)=0,\ y''(0)=0.
\end{aligned} \tag{16}$$

The exact/true solution of the equation (16) is and the fitness/error function of above equation is given below:

$$\begin{aligned}
\varepsilon=&\frac{1}{N}\sum_{m=1}^{N}\left(t_m^2\hat{y}'''(t_m)+4t_m\hat{y}''(t_m)+2\hat{y}'(t_m)-9t_m^2(4+10t_m^3+3t_m^6)\hat{y}\right)^2+ \\
&\frac{1}{3}\left(\left(\hat{y}_0-1\right)^2+\left(\hat{y}_0'\right)^2+\left(\hat{y}_0''\right)\right)
\end{aligned} \tag{17}$$

Case-3:

Using $p=3$ and $f(t)g(y)=-6(10+2t^3+6t^6)e^{-3y}$ in equation (1). The nonlinear Emden-Fowler equation takes the form as:

$$\mathrm{y}'''(\mathrm{t}) + \left(\frac{6}{t}\right) y''(t) + \left(\frac{6}{t^2}\right) y'(t) - 6(10 + 2t^3 + 6t^6)e^{-3y} = 0$$

$$y(0) = 0, \;\; y'(0) = y''(0) = 0. \tag{18}$$

The exact/true solution of the equation (18) is $\log(1+t^3)$ and the fitness formulation of above case is written as:

$$\varepsilon = \frac{1}{N}\sum_{m=1}^{N}\left(t_m^2 \hat{y}'''(t_m) + 6t_m \hat{y}''(t_m) + 6\hat{y}'(t_m) - 6t_m^2(10 + 2t_m^3 + 6t_m^6)e^{-3\hat{y}}\right)^2 +$$
$$\frac{1}{3}\left(\left(\hat{y}_0\right)^2 + \left(\hat{y}_0'\right)^2 + \left(\hat{y}_0''\right)\right) \tag{19}$$

Case-4:

Take $p = 4$, $g(y) = y^m$ and $f(t) = 1$ in equation (1) using $m = 0$. The Lane-Emden nonlinear model becomes as:

$$\mathrm{y}'''(\mathrm{t}) + \left(\frac{8}{t}\right) y''(t) + \left(\frac{12}{t^2}\right) y'(t) + y^m = 0\,,$$

$$y(0) = 1, \;\; y'(0) = 0, \;\;\; y''(0) = 0. \tag{20}$$

The true solution of the model (20) is $1 - \frac{1}{90}t^3$ and error function becomes as:

$$\varepsilon = \frac{1}{N}\sum_{m=1}^{N}\left(t_m^2 \hat{y}'''(t_m) + 8t_m \hat{y}''(t_m) + 12\hat{y}'(t_m) + t_m^2 \hat{y}^m\right)^2 + \frac{1}{3}\left(\left(\hat{y}_0 - 1\right)^2 + \left(\hat{y}'\right)^2 + \left(\hat{y}_0''\right)^2\right) \tag{21}$$

Case-5:

By taking $p = 4$ and $g(y) = -(10 + 10t^3 + t^6)y$ in equation (1), The Emden-Fowler equation becomes as:

$$\mathrm{y}'''(\mathrm{t}) + \left(\frac{4}{t}\right) y''(t) - (t^6 + 10t^3 + 10)y = 0,$$

$$y(0) = 1, \;\; y'(0) = 0, \;\; y''(0) = 0. \tag{22}$$

The true solution of the equation (23) is $e^{\frac{t^3}{3}}$ and error function becomes as:

$$\varepsilon = \frac{1}{N}\sum_{m=1}^{N}\left(t_m \hat{y}'''(t_m) + 4\hat{y}''(t_m) - t_m(10 + 10t_m^3 + t_m^6\right)^2 \hat{y} + \frac{1}{3}\left(\left(\hat{y}_0 - 1\right)^2 + \left(\hat{y}_0'\right)^2 + \left(\hat{\boldsymbol{y}}_{\boldsymbol{0}}''\right)^2\right) \tag{23}$$

Optimization is performed for all five cases supported by the GA-ASA for 100 independent runs. Set of weights and comparison of results performance measure of GA-ASA are graphically presented in Fig. 2 and 3. It is clear that the best and mean solutions are overlapped with the true solutions for all cases. To find the similarities of the results, the graphs of AE from exact solutions are plotted in Fig. 3. The values of AE lie around10^{-06} to 10^{-07}, 10^{-04} to 10^{-05}, 10^{-06} to 10^{-08}, 10^{-06} to $10^{-09}$and 10^{-07} to 10^{-09} for best solution, 10^{-02} to 10^{-03}, 10^{-01} to 10^{-02}, 10^{-02} to 10^{-03}, $10^{-02}$to 10^{-04} and 10^{-04} to 10^{-05} for mean solution and for even for worst solution the AE lie around10^{-01} to 10^{-02}, 10^{00} to 10^{-01}, 10^{-01} to 10^{-02}, 10^{-02} to 10^{-05} and 10^{-03} to 10^{-04} for all the cases. Performance indices for all cases are plotted in Fig3. The values of MAD lie around 10^{-06} to 10^{-08}, 10^{-04} to 10^{-06}, 10^{-04} to 10^{-06}, 10^{-06} to 10^{-08} and 10^{-05} to 10^{-07},while the values of TIC lie around 10^{-10} to 10^{-12}, 10^{-08} to 10^{-10}, 10^{-08} to 10^{-09}, 10^{-11} to$10^{-12}$and 10^{-11} to 10^{-14} for best solution. Moreover, the best values of ENSE lie between10^{-12} to 10^{-14}, 10^{-09} to 10^{-10}, 10^{-09} to 10^{-10}, 10^{-11} to 10^{-12}, and 10^{-13} to 10^{-15}. The mean values of MAD lie around 10^{-02} to 10^{-04}, 10^{-02} to 10^{-04}, 10^{-02} to 10^{-03}, 10^{-02} to10^{-04}, and 10^{-01} to 10^{-03}. Whereas, the mean values of TIC lie between 10^{-06} to 10^{-08},10^{-06} to 10^{-07}, 10^{-07} to 10^{-08}, 10^{-06} to 10^{-08} and 10^{-06} to 10^{-08} and the values of ENSE lie between 10^{-03} to 10^{-04}, 10^{-02} to 10^{-04}, 10^{-03} to 10^{-04}, 10^{-02} to 10^{-04}, and 10^{-01} to10^{-05}. The worst values of MAD lie around 10^{-01} to 10^{-02}, 10^{-01} to 10^{-02}, 10^{-01} to 10^{-02},10^{-03} to 10^{-04} and 10^{-01} to 10^{-03}. Whereas, the worst values of TIC lie between 10^{-04} to10^{-05}, 10^{-02} to 10^{-04}, 10^{-02} to 10^{-04}, 10^{-06} to 10^{-08} and 10^{-04} to $10^{-05}$and the values of ENSE lie between 10^{-02} to 10^{-03}, 10^{02} to 10^{00}, 10^{00} to 10^{-01}, 10^{-04} to $10^{-05}$and $10^{-01}$to 10^{-02}. Graphical representation of statistical analyses along with the histograms is shown in Figs. 4 and 5 for all five cases. The convergence analysis of the fitness values TIC, MAD and ENSE achieved for a number of independent runs. The result shows that almost 80% runs attain precise values of TIC, MAD and ENSE.

For more precision of the designed scheme, statistical analysis is performed in the terms of minimum (Min), mean (Mean) and standard deviation (S.D). These statistical values for cases 1, 2, 3, 4 and 5 are tabulated in Table 2 for $\hat{y}(x)$. The Min values for all the cases lie in the ranges of [10^{-07}, 10^{-08}] for case 1, [10^{-05}, 10^{-06}] for case 2, [10^{-06}, 10^{-08}] for case 3, [10^{-08}, 10^{-10}] for case 4 and [10^{-07}, 10^{-09}] for case 5, whereas, the Mean values mostly lie in the ranges of [10^{-02}, 10^{-03}] but in some cases it goes up to [10^{-05}, 10^{-06}] as well. Moreover, the S.D values prove very good ranges and lie in good ranges for all the cases. The global performance operators shown as [GFIT, GMAD, GTIC, GENSE] for 100 execution are tabulated in Table 3 for all five cases. The magnitude (Mag) and S.D proved very good results for the global statistical operators [GFIT, GMAD, GTIC, GENSE].

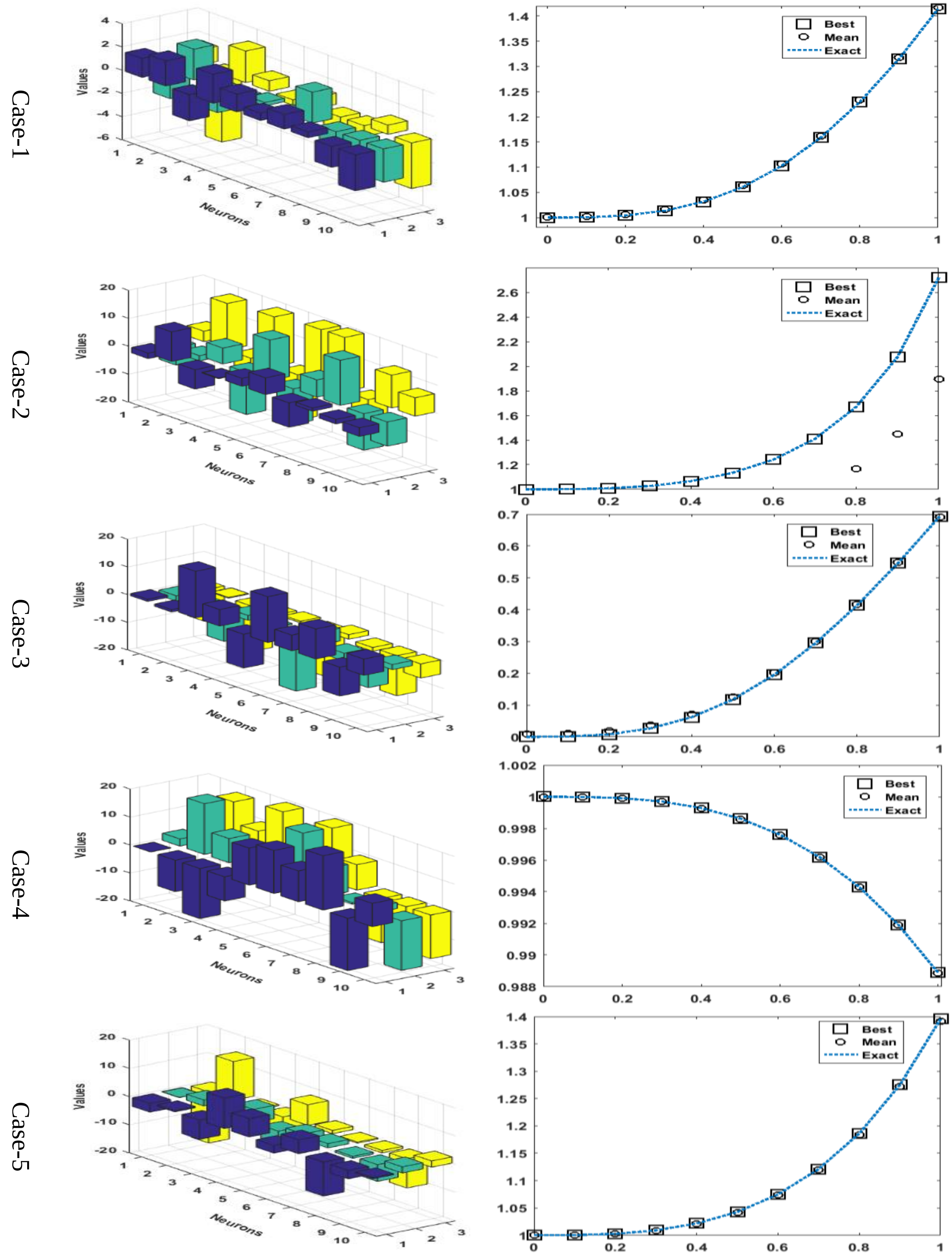

Fig 2: Set of weights, comparison of results for all cases

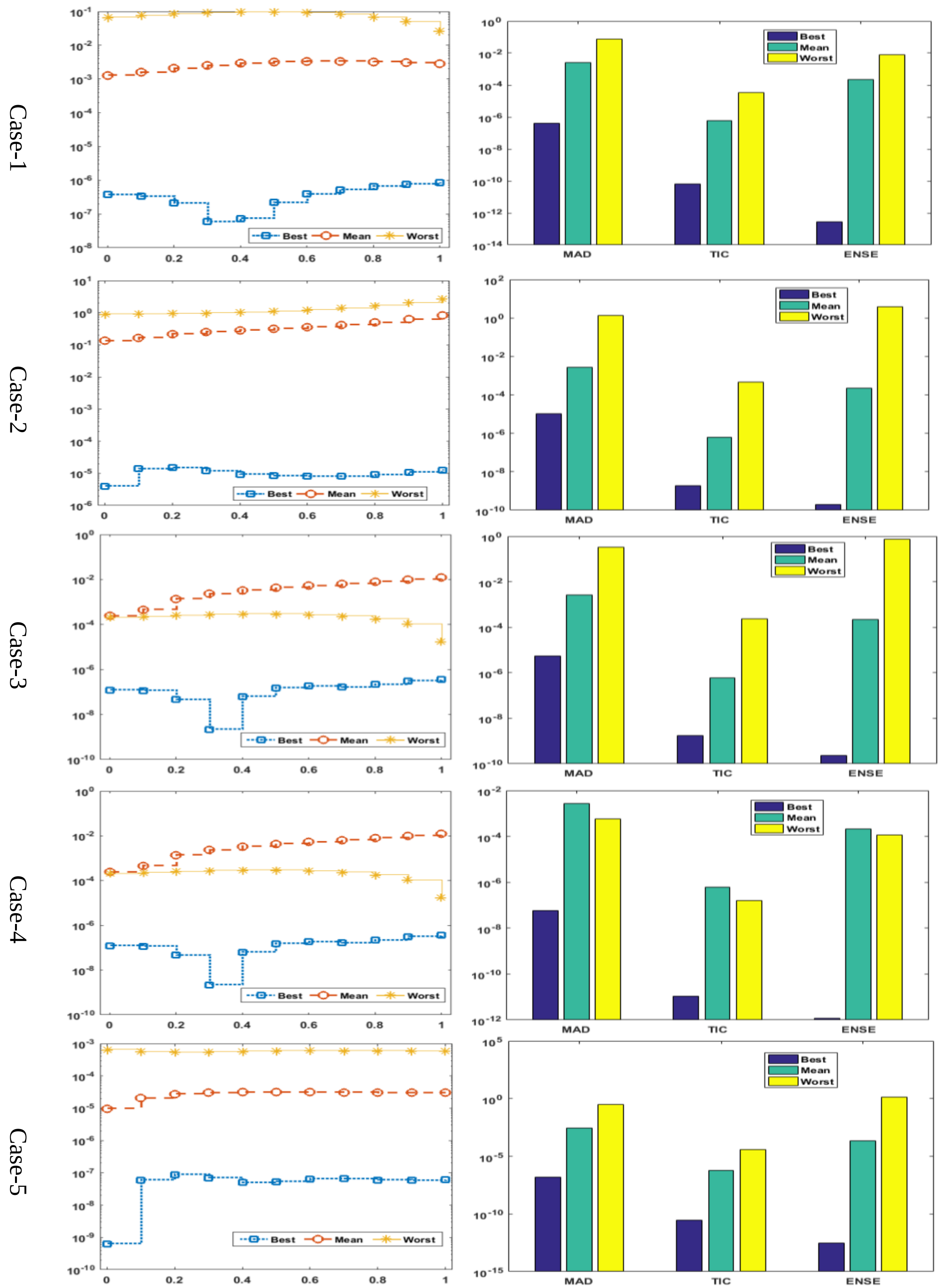

Fig 3: AE and performance measure for all cases

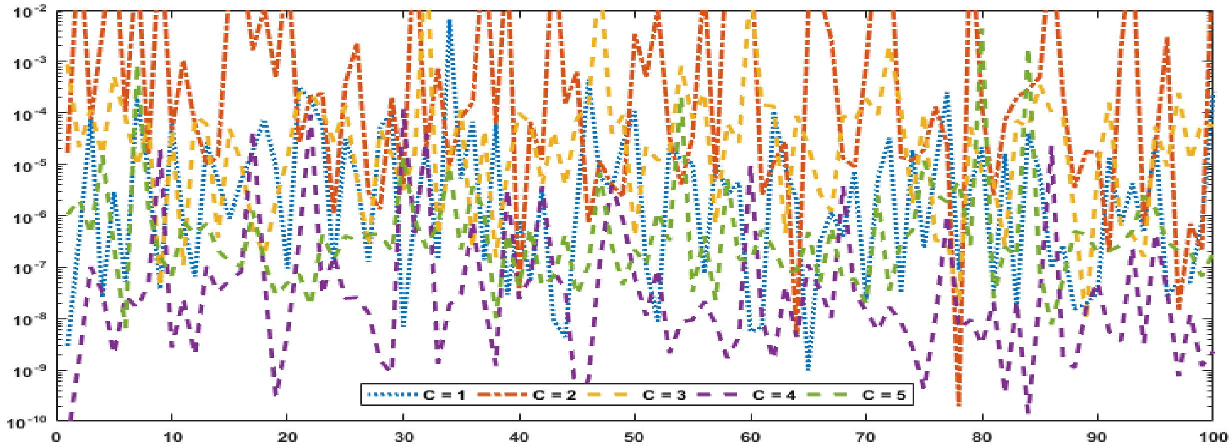

Fitness value in convergence analysis for Cases 1 to 5

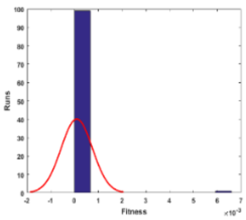

(a) Histogram for Case 1

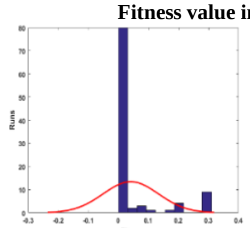

(b) Histogram for Case2

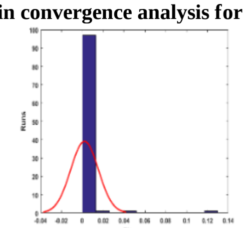

(c) Histogram for Case 3

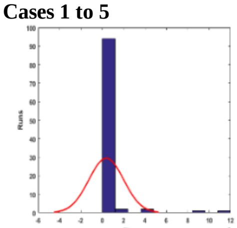

(d) Histogram for Case 4

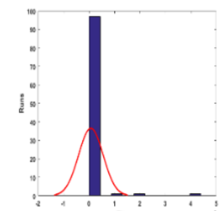

(e) Histogram for Case 5

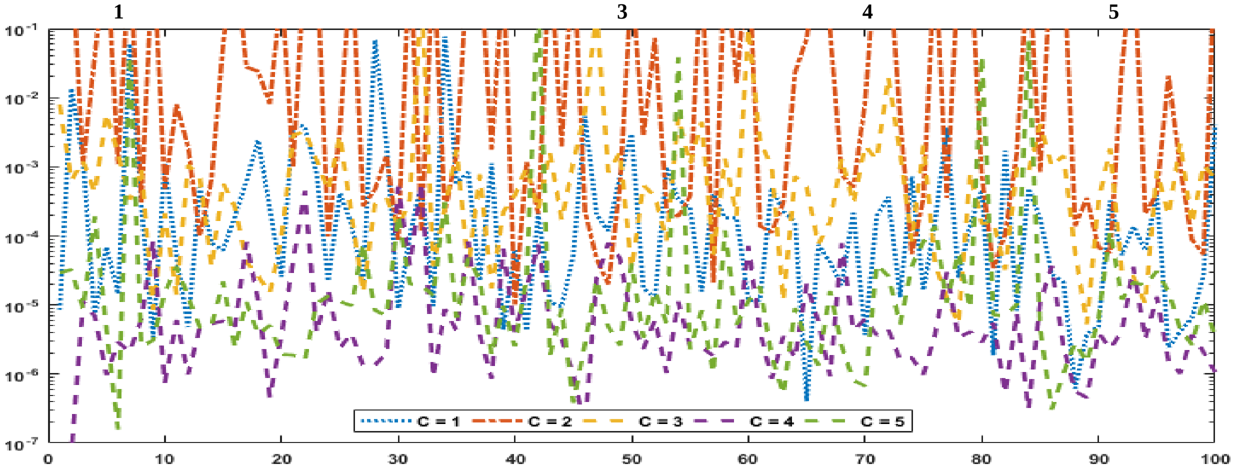

MAD value in convergence analysis for Cases 1 to 5

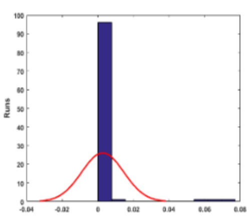

(a) Histogram for Case 1

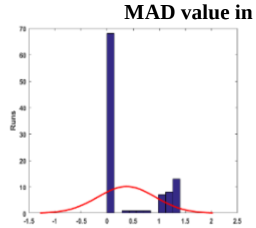

(b) Histogram for Case 2

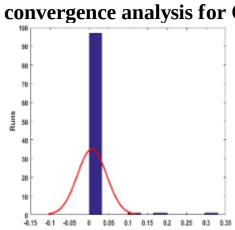

(c) Histogram for Case 3

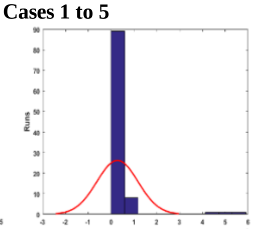

(d) Histogram for Case 4

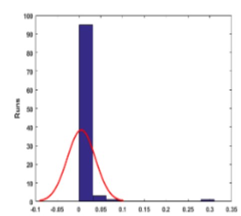

(e) Histogram for Case 5

Fig 4: Fitness values, MAD values and Histogram of GA-ASA for all Cases

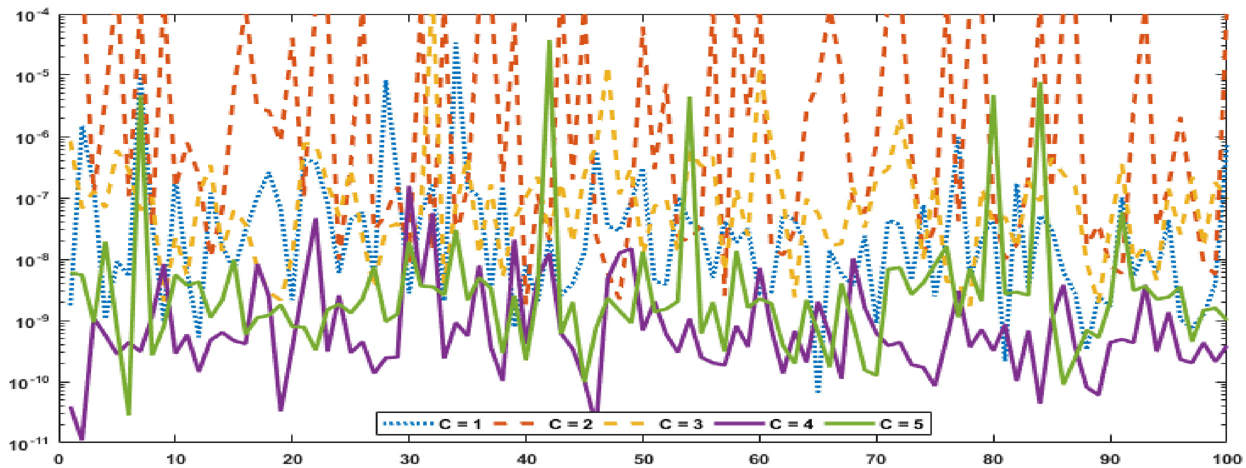

TIC value in convergence analysis for Cases 1 to 5

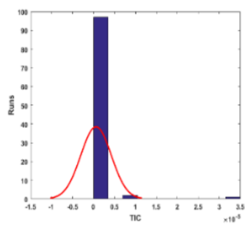

(a) Histogram for Case 1

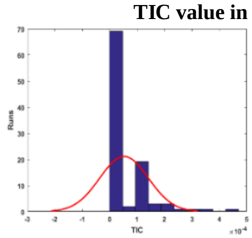

(b) Histogram for Case 2

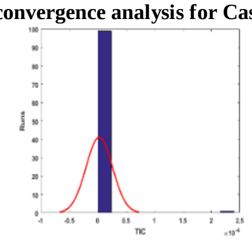

(c) Histogram for Case 3

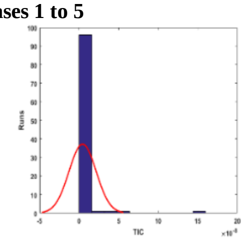

(d) Histogram for Case 4

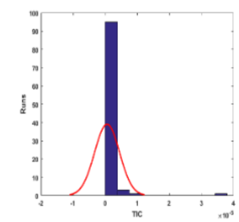

(e) Histogram for Case 5

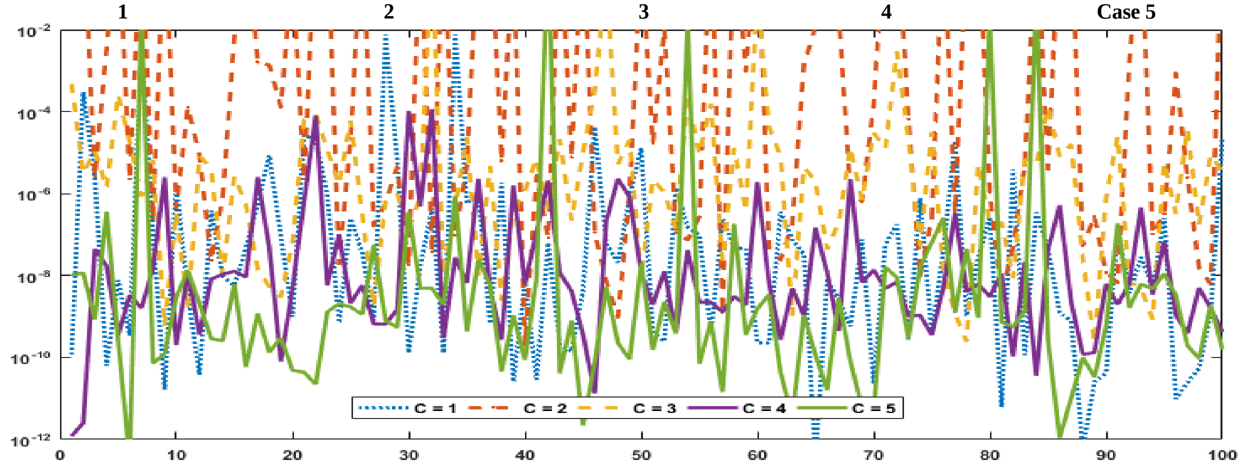

ENSE value in convergence analysis for Cases 1 to 5

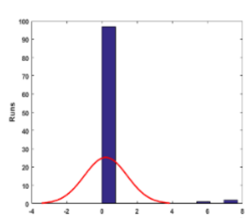

(a) Histogram for Case 1

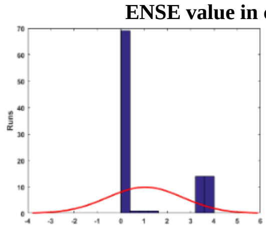

(b) Histogram for Case 2

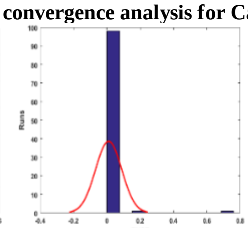

(c) Histogram for Case 3

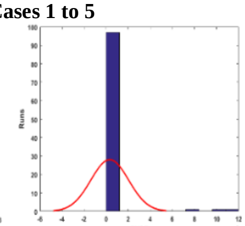

(d) Histogram for Case 4

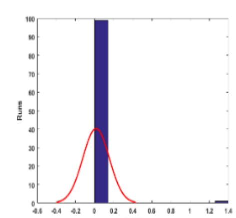

(e) Histogram for Case 5

Fig 5: TIC values, ENSE values and Histogram of GA-ASA for all Cases

Table 2: Statistics results for all cases of singular model

x	Case-1			Case-2			Case-3			Case-4			Case-5		
	Min	**Mean**	**S.D**	**Min**	**Mean**	**S.D**	**Min**	**Mean**	**S.D**	**Min**	**Mean**	**S.D**	**Min**	**Mean**	**S.D**
0	3.2E-08	1.3E-03	6.8E-03	4.0E-06	1.3E-01	2.8E-01	1.7E-07	1.0E-02	5.3E-02	1.5E-10	9.6E-06	6.5E-05	6.5E-08	2.3E-04	1.4E-03
0.1	1.1E-08	1.6E-03	7.8E-03	1.4E-05	1.7E-01	2.9E-01	2.6E-07	1.0E-02	5.4E-02	2.9E-08	2.1E-05	6.3E-05	1.1E-07	4.6E-04	3.1E-03
0.2	2.1E-07	2.1E-03	9.3E-03	9.0E-06	2.2E-01	3.4E-01	9.3E-06	1.1E-02	5.4E-02	7.9E-08	2.7E-05	7.4E-05	4.6E-08	1.4E-03	9.2E-03
0.3	6.0E-08	2.5E-03	1.1E-02	3.6E-06	2.5E-01	3.8E-01	9.2E-06	1.0E-02	5.3E-02	6.7E-08	3.0E-05	9.0E-05	2.1E-09	2.4E-03	1.5E-02
0.4	5.1E-08	2.9E-03	1.2E-02	2.2E-06	3.0E-01	4.2E-01	8.8E-06	9.6E-03	5.0E-02	4.9E-08	3.3E-05	1.2E-04	2.0E-08	3.4E-03	1.9E-02
0.5	2.2E-07	3.1E-03	1.5E-02	1.5E-06	3.3E-01	4.8E-01	7.5E-06	8.5E-03	4.6E-02	5.4E-08	3.3E-05	1.3E-04	8.5E-08	4.4E-03	2.8E-02
0.6	2.7E-07	3.5E-03	1.6E-02	8.1E-06	3.6E-01	5.3E-01	5.5E-06	7.0E-03	3.9E-02	6.5E-08	3.2E-05	1.1E-04	2.5E-08	5.4E-03	3.4E-02
0.7	3.7E-07	3.5E-03	1.7E-02	4.8E-06	4.2E-01	6.3E-01	3.1E-06	5.0E-03	3.0E-02	6.7E-08	3.2E-05	1.1E-04	2.1E-08	6.5E-03	4.1E-02
0.8	2.3E-07	3.2E-03	1.6E-02	9.1E-06	5.0E-01	7.4E-01	4.1E-08	2.9E-03	2.0E-02	3.6E-08	3.0E-05	1.0E-04	7.8E-08	8.2E-03	5.3E-02
0.9	1.3E-08	3.0E-03	1.7E-02	1.2E-05	6.3E-01	9.3E-01	9.2E-07	1.6E-03	1.0E-02	5.9E-08	3.1E-05	1.0E-04	7.7E-08	1.0E-02	7.7E-02
1	2.4E-07	2.9E-03	1.4E-02	1.3E-05	8.3E-01	1.3E+00	4.2E-06	1.9E-03	6.5E-03	3.1E-08	3.0E-05	1.1E-04	2.8E-07	1.2E-02	8.3E-02

Table 3: Global performance results for all five cases

Index	Cases	GFIT		GMAD		GTIC		GENSE	
		Mag	**S.D**	**Mag**	**S.D**	**Mag**	**S.D**	**Mag**	**S.D**
$\hat{y}(x)$	1	9.4E-05	6.7E-04	2.8E-03	1.3E-02	6.1E-07	3.7E-06	2.2E-04	1.3E-03
	2	4.3E-02	9.3E-02	3.7E-01	5.6E-01	5.2E-05	9.0E-05	1.1E+00	1.7E+00
	3	1.9E-03	1.4E-02	7.2E-03	3.8E-02	2.8E-06	2.4E-05	1.1E-02	8.0E-02
	4	3.8E-06	1.7E-05	2.9E-05	8.9E-05	4.4E-09	1.8E-08	3.2E-06	1.8E-05
	5	7.6E-05	5.0E-04	5.0E-03	3.2E-02	5.9E-07	3.9E-06	1.6E-02	1.5E-01

4. Conclusion

The motivation behind this study is to solve third order nonlinear singular differential model by exploiting the strength of integrated intelligent computing paradigm based on artificial neural network models optimized with genetic algorithm hybrid with active-set technique. Some of the key findings are summarized below

- Artificial neural network successfully applied to solve the third order nonlinear singular differential model.
- The accuracy and convergence of the present method are analyzed through the outcomes of statistical measures based on 100 independent runs to solve five cases of third order nonlinear singular differential model.

- The best AE values lie up to 10^{-05} to 10^{-09}. However, the worst solution of AE also lie upto 10^{-01} to 10^{-05}.
- The global FIT, MAD, TIC and ENSE are presented with good agreements with their optimal gauges.

In future, the present technique will be applied for solving the higher order nonlinear singular system represented with partial differential equations.

5. Acknowledgments: This paper has been partially supported by Ministerio de Ciencia, Innovación y Universidades grant number PGC2018-097198-B-I00 and Fundación Séneca de la Región de Murcia grant number 20783/PI/18.

References

[1] Lane, H.J., 1870. On the Theoretical Temperature of the Sun, under the Hypothesis of a gaseous Mass maintaining its Volume by its internal Heat and depending on the laws of gases as known to terrestrial Experiment. American Journal of Science, (148), pp. 57-74.

[2] Emden, R., 1907. Gaskugeln Teubner. Leipzig und Berlin

[3] Ahmad, I., Raja, M. A. Z., Bilal, M. and Ashraf, F., 2016. Neural network methods to solve the Lane–Emden type equations arising in thermodynamic studies of the spherical gas cloud model. Neural Computing and Applications, pp. 1-16.

[4] Mandelzweig, V. B. and Tabakin, F., 2001. Quasi linearization approach to nonlinear problems in physics with application to nonlinear ODEs. Computer Physics Communications, 141(2), pp. 268-281.

[5] Luo, T., Xin, Z. and Zeng, H., 2016. Nonlinear asymptotic stability of the Lane-Emden solutions for the viscous gaseous star problem with degenerate density dependent viscosities. Communications in Mathematical Physics, 347(3), pp. 657-702.

[6] Rach, R., Duan, J. S. and Wazwaz, A. M., 2014. Solving coupled Lane–Emden boundary value problems in catalytic diffusion reactions by the Adomian decomposition method. Journal of Mathematical Chemistry, 52(1), pp. 255-267.

[7] Boubaker, K. and Van Gorder, R.A., 2012. Application of the BPES to Lane–Emden equations governing polytropic and isothermal gas spheres. New Astronomy, 17(6), pp. 565-569.

[8] Rach, R., Duan, J. S. and Wazwaz, A. M., 2014. Solving coupled Lane–Emden boundary value problems in catalytic diffusion reactions by the Adomian decomposition method. Journal of Mathematical Chemistry, 52(1), pp. 255-267

[9] Taghavi, A., Pearce, S., 2013. A solution to the Lane–Emden equation in the theory of stellar structure utilizing the Tau method. Mathematical Methods in the Applied Sciences, 36(10), pp.1240-1247.

[10] Khan, J. A., Raja, M. A. Z., Rashidi, M. M., Syam, M. I. and Wazwaz, A. M., 2015. Nature-inspired computing approach for solving non-linear singular Emden–Fowler problem arising in electromagnetic theory. Connection Science, 27(4), pp. 377-396.

[11] Bhrawy, A. H., Alofi, A. S. and Van Gorder, R. A., 2014, May. An efficient collocation method for a class of boundary value problems arising in mathematical physics and geometry. In Abstract and Applied Analysis (Vol. 2014). Hindawi Publishing Corporation.

[12] Ramos, J. I., 2003. Linearization methods in classical and quantum mechanics. Computer Physics Communications, 153(2), pp. 199-208.

[13] Dehghan, M. and Shakeri, F., 2008. Solution of an integro-differential equation arising in oscillating magnetic fields using He's homotopy perturbation method. Progress in Electromagnetics Research, 78, pp. 361-376.

[14] Radulescu, V. and Repovs, D., 2012. Combined effects in nonlinear problems arising in the study of anisotropic continuous media. Nonlinear Analysis: Theory, Methods and Applications, 75(3), pp. 1524-1530.

[15] Flockerzi, D. and Sundmacher, K., 2011. On coupled Lane-Emden equations arising in dusty fluid models. In Journal of Physics: Conference Series (Vol. 268, No. 1, p. 012006). IOP Publishing.

[16] Ghergu, M. and Radulescu, V., 2007. On a class of singular Gierer–Meinhardt systems arising in morphogenesis. Comptes Rendus Mathématique, 344(3), pp. 163-168.

[17] Bender, C. M., Milton, K. A., Pinsky, S. S. and Simmons Jr, L. M., 1989. A new perturbative approach to nonlinear problems. Journal of Mathematical Physics, 30(7), pp. 1447-1455.

[18] Shawagfeh, N. T., 1993. Non perturbative approximate solution for Lane–Emden equation. Journal of Mathematical Physics, 34(9), pp. 4364-4369.

[19] Wazwaz, A. M., 2001. A new algorithm for solving differential equations of Lane–Emden type. Applied Mathematics and Computation, 118(2), pp. 287-310.

[20] Liao, S., 2003. A new analytic algorithm of Lane–Emden type equations. Applied Mathematics and Computation, 142(1), pp. 1-16.

[21] Parand, K. and Razzaghi, M., 2004. Rational Legendre approximation for solving some physical problems on semi-infinite intervals. Physica Scripta, 69(5), p. 353.

[22] Nouh, M.I., 2004. Accelerated power series solution of polytropic and isothermal gas spheres. New Astronomy, 9(6), pp. 467-473.

[23] Mandelzweig, V.B. and Tabakin, F., 2001. Quasilinearization approach to nonlinear problems in physics with application to nonlinear ODEs. Computer Physics Communications, 141(2), pp. 268-281.

[24] Burke, E. K., Gendreau, M., Hyde, M., Kendall, G., Ochoa, G., Ozcan, E. and Qu, R., 2013. Hyper-heuristics: A survey of the state of the art. Journal of the Operational Research Society, 64(12), pp. 1695-1724.

[25] Chen, H., Jiang, J., Cao, D. and Fan, X., 2018. Numerical investigation on global dynamics for nonlinear stochastic heat conduction via global random attractor's theory. Applied Mathematics and Nonlinear Sciences, 3(1), pp.175-186.

[26] Motyl, J., 2017. Upper separated multifunctions in deterministic and stochastic optimal control. Applied Mathematics and Nonlinear Sciences, 2(2), pp.479-484.

[27] Raja, M. A. Z., Zameer, A., Khan, A.U. and Wazwaz, A.M., 2016. A new numerical approach to solve Thomas–Fermi model of an atom using bio-inspired heuristics integrated with sequential quadratic programming. Springer Plus, 5(1), p. 1400.

[28] Umar, M., Sabir, Z. and Raja, M.A.Z., 2019. Intelligent computing for numerical treatment of nonlinear prey–predator models. Applied Soft Computing, 80, pp.506-524.

[29] Raja, M. A. Z., Shah, F. H., Tariq, M. and Ahmad, I., 2016. Design of artificial neural network models optimized with sequential quadratic programming to study the dynamics of nonlinear Troesch's problem

[30] Zhang, Z., El-Moselhy, T. A., Elfadel, I. M. and Daniel, L., 2013. Stochastic testing method for transistor-level uncertainty quantification based on generalized polynomial chaos. IEEE Transactions on Computer-Aided Design of Integrated Circuits and Systems, 32(10), pp. 1533-1545.

[31] Raja, M. A. Z., Shah, F. H., Alaidarous, E. S. and Syam, M. I., 2017. Design of bio-inspired heuristic technique integrated with interior-point algorithm to analyze the dynamics of heartbeat model. Applied Soft Computing, 52, pp. 605-629.

[32] Sharma, G., Friedenberg, D. A., Annetta, N., Glenn, B., Bockbrader, M., Majstorovic, C., Domas, S., Mysiw, W. J., Rezai, A. and Bouton, C., 2016. Using an Artificial Neural Bypass to Restore Cortical Control of Rhythmic Movements in a Human with Quadriplegia. Scientific Reports, 6.

[33] He, W., Chen, Y. and Yin, Z., 2016. Adaptive neural network control of an uncertain robot with full-state constraints. IEEE Transactions on Cybernetics, 46(3), pp. 620-629.

[34] Schaff, J. C., Gao, F., Li, Y., Novak, I. L. and Slepchenko, B. M., 2016. Numerical Approach to Spatial Deterministic-Stochastic Models Arising in Cell Biology. PLoS computational biology, 12(12), p. e1005236.

[35] Pelletier, F., Masson, C. and Tahan, A., 2016. Wind turbine power curve modelling using artificial neural network. Renewable Energy, 89, pp. 207-214.

[36] Manik, S., Saini, L. M. and Vadera, N., 2016, July. Counting and classification of white blood cell using Artificial Neural Network (ANN). In Power Electronics, Intelligent Control and Energy Systems (ICPEICES), IEEE International Conference on (pp. 1-5). IEEE.

[37] Wazwaz, A. M., 2015. Solving two Emden-Fowler type equations of third order by the variational iteration method. Applied Mathematics and Information Sciences, 9(5), p. 2429.

[38] Yadav, A. K. and Chandel, S. S., 2014. Solar radiation prediction using Artificial Neural Network techniques: A review. Renewable and sustainable energy reviews, 33, pp. 772-781.

[39] Cortes, C., Gonzalvo, X., Kuznetsov, V., Mohri, M. and Yang, S., 2016. Adanet: Adaptive structural learning of artificial neural networks. arXiv preprint arXiv:1607.01097.

[40] Ebrahimi, E., Monjezi, M., Khalesi, M. R. and Armaghani, D. J., 2016. Prediction and optimization of back-break and rock fragmentation using an artificial neural network and a bee colony algorithm. Bulletin of Engineering Geology and the Environment, 75(1), pp. 27-36.

[41] Zalzala, A. M., 1997. Genetic algorithms in engineering systems (Vol. 55). Iet.

[42] Srinivas, N. and Deb, K., 1994. Muilti-objective optimization using no dominated sorting in genetic algorithms. Evolutionary computation, 2(3), pp. 221-248.

[43] Sridhar, R., M. Chandrasekaran, C. Sriramya, and Tom Page. "Optimization of heterogeneous Bin packing using adaptive genetic algorithm." In IOP Conference Series: Materials Science and Engineering, vol. 183, no. 1, p. 012026. IOP Publishing, 2017.

[44] Chang, F. S., 2016. Greedy-Search-based Multi-Objective Genetic Algorithm for Emergency Humanitarian Logistics Scheduling.

[45] An, P. Q., Murphy, M. D., Breen, M.C. and Scully, T., 2016, August. One-day-ahead cost optimisation for a multi-energy source building using a genetic algorithm. In Control (CONTROL), 2016 UKACC 11th International Conference on (pp. 1-6). IEEE.

[46] Vaishnav, P., Choudhary, N. and Jain, K., 2017. Traveling Salesman Problem Using Genetic Algorithm: A Survey.

[47] Das, S., Chaudhuri, S. and Das, A.K., 2017, February. Optimal Set of Overlapping Clusters Using Multi-objective Genetic Algorithm. In Proceedings of the 9th International Conference on Machine Learning and Computing (pp. 232-237). ACM.

[48] Tuhus-Dubrow, D. and Krarti, M., 2010. Genetic-algorithm based approach to optimize building envelope design for residential buildings. Building and environment, 45(7), pp. 1574-1581.

[49] Azad, A.V. and Azad, N.V., 2016. Application of nanofluids for the optimal design of shell and tube heat exchangers using genetic algorithm. Case Studies in Thermal Engineering, 8, pp.198-206.

[50] Alharbi, S. and Venkat, I., 2017. A genetic algorithm based approach for solving the minimum dominating set of queens problem. Journal of Optimization, 2017.

[51] Hoque, M. S., Mukit, M., Bikas, M. and Naser, A., 2012. An implementation of intrusion detection system using genetic algorithm. arXiv preprint arXiv: 1204.1336.

[52] Tan, J. and Kerr, W. L., 2017. Determination of glass transitions in boiled candies by capacitance based thermal analysis (CTA) and genetic algorithm (GA). Journal of Food Engineering, 193, pp. 68-75.

[53] Ball, M. G., Qela, B. and Wesolkowski, S., 2016. A Review of the Use of Computational Intelligence in the Design of Military Surveillance Networks. In Recent Advances in Computational Intelligence in Defense and Security (pp. 663-693). Springer International Publishing.

[54] You, C., Li, C. G., Robinson, D. P. and Vidal, R., 2016. Oracle based active set algorithm for scalable elastic net subspace clustering. In Proceedings of the IEEE Conference on Computer Vision and Pattern Recognition (pp. 3928-3937).

[55] Myre, J. M., Frahm, E., Lilja, D.J. and Saar, M.O., 2017. TNT-NN: A Fast Active Set Method for Solving Large Non-Negative Least Squares Problems. Procedia Computer Science, 108, pp. 755-764.

[56] Koehler, S., Danielson, C. and Borrelli, F., 2017. A primal-dual active-set method for distributed model predictive control. Optimal Control Applications and Methods, 38(3), pp. 399-419.

[57] Wang, X. and Pardalos, P. M., 2017. A modified active set algorithm for transportation discrete network design bi-level problem. Journal of Global Optimization, 67(1-2), pp. 325-342.

[58] Shen, C., Zhang, L. H. and Yang, W. H., 2016. A Filter Active-Set Algorithm for Ball/Sphere Constrained Optimization Problem. SIAM Journal on Optimization, 26(3), pp. 1429-1464.